European Journal of Medicinal Chemistry 209 (2021) 112875

Contents lists available at ScienceDirect

European Journal of Medicinal Chemistry

journal homepage: http://www.elsevier.com/locate/ejmech

Research paper

Ninhydrins inhibit carbonic anhydrases directly binding to the metal ion

Abdeslem Bouzina [a, b, 1], Malika Berredjem [b], Alessio Nocentini [c, d, 1], Silvia Bua [c], Zouhair Bouaziz [a], Joachim Jose [e], Marc Le Borgne [a, f], Christelle Marminon [a, f, **], Paola Gratteri [c, d, *], Claudiu T. Supuran [c]

[a] EA 4446 Bioactive Molecules and Medicinal Chemistry, Faculté de Pharmacie-ISPB, SFR Santé Lyon-Est CNRS UMS3453-INSERM US7, Université de Lyon, Université Claude Bernard Lyon 1, 8 Avenue Rockefeller, F-69373, Lyon Cedex 8, France
[b] Laboratory of Applied Organic Chemistry, Synthesis of Biomolecules and Molecular Modelling Group, Badji-Mokhtar-Annaba University, Box 12, Annaba, 23000, Algeria
[c] Department of NEUROFARBA, Section of Pharmaceutical and Nutraceutical Sciences, University of Florence, Florence, Italy
[d] Department of NEUROFARBA, Section of Pharmaceutical and Nutraceutical Sciences, Laboratory of Molecular Modeling Cheminformatics & QSAR, University of Florence, Florence, Italy
[e] Institute of Pharmaceutical and Medicinal Chemistry, PharmaCampus, Westfälische WilhelmsUniverstität Münster, 48149, Münster, Germany
[f] Small Molecules for Biological Targets Team, Centre de recherche en cancérologie de Lyon, Centre Léon Bérard, CNRS 5286, INSERM 1052, Université Claude Bernard Lyon 1, Univ Lyon, Lyon, 69373, France

ARTICLE INFO

Article history:
Received 30 July 2020
Received in revised form
27 August 2020
Accepted 22 September 2020
Available online 5 October 2020

Keywords:
Carbonic anhydrases
Ninhydrins
Microwave synthesis
Inhibitors
Binding mode
Zinc binder

ABSTRACT

Ninhydrins show extensive application in organic chemistry and agriculture whereas they have been poorly investigated as bioactive molecules for medicinal chemistry purposes. A series of ninhydrin derivatives was here investigated for the inhibition of human carbonic anhydrases (CAs, EC 4.2.1.1), based on earlier evidence that gem diols are able to coordinate the metal ion from the CA active site. Ninhydrins demonstrated a micromolar inhibitory action against CA I and IX (K_Is in the range 0.57–68.2 μM) and up to a nanomolar efficacy against CA II and VII (K_Is in the range 0.025–78.2 μM), validated isoforms as targets in several CNS-related diseases. CA IV was instead weakly or poorly inhibited. A computational protocol based on docking, MM-GBSA and metadynamics calculations was used to elucidate the putative binding mode of this type of inhibitors to CA II and CA VII. The findings of this study testify that such pharmacologically underestimated ligands may represent interesting lead compounds for the development of CA inhibitors possessing an innovative mechanism of action, i.e., mono- or bis-coordination to the zinc ion through the diol moiety.

1. Introduction

Carbonic anhydrases (CAs, EC 4.2.1.1), a group of ubiquitously expressed metalloenzymes, are implicated in numerous physiological and pathological processes. Fifteen different CA isoforms have been identified and characterized in human (h) so far [1,2]. A chorus of chemotypes have been evaluated for the design of hCAs inhibitors or activators with biomedical applications [3]. On the basis of previous exploratory work on the inhibitory action of a gem diol derivative (bearing a trifluoro-dihydroxy-propanone moiety) which was observed to coordinated to the metal ion from the CA active site [3] and in order to explore a new molecular scaffold capable of interacting with CAs in the same manner, ninhydrin (2,2-dihydroxyindane-1,3-dione, CAS number 485-47-2) and some of its substituted derivatives were selected for detailed investigations. It should be stressed here that ninhydrins were not investigated so far as inhibitors of CAs.

On 1910, S. Ruhemann described for the very first time the synthesis of ninhydrin and its particular reactivity towards amines

* Corresponding author. Department of NEUROFARBA, Section of Pharmaceutical and Nutraceutical Sciences, University of Florence, Florence, Italy.
** Corresponding author. EA 4446 Bioactive Molecules and Medicinal Chemistry, Faculté de Pharmacie-ISPB, SFR Santé Lyon-Est CNRS UMS3453-INSERM US7, Université de Lyon, Université Claude Bernard Lyon 1, 8 Avenue Rockefeller, F-69373, Lyon Cedex 8, France.
E-mail addresses: christelle.marminon-davoust@univ-lyon1.fr (C. Marminon), paola.gratteri@unifi.it (P. Gratteri).
[1] These investigators equally contributed to the work.

https://doi.org/10.1016/j.ejmech.2020.112875
0223-5234/

Abbreviations

AAZ	acetazolamide
BCS	Binding CompScore
BP	Binding Persistence
BP	Binding pose
BPS	Binding PoseScore
CAs	Carbonic anhydrases
h	human
HMBC	Heteronuclear Multiple Bond Correlation
MM-GBSA	Molecular Mechanics-Generalized Born Surface Area
NOE	Nuclear Overhauser Effect
NOESY	Nuclear Overhauser Effect Spectroscopy
RMDS	Reactive Molecular Dynamics Simulation
RMSD	Root Mean Square Deviation
SAR	structure-activity relationship
TBID	tetrabromoindane-1,3-dione
VSGB	variable dielectric surface generalized born

and ammonia, yielding colored products [4]. Ninhydrin is sensitive to prolonged exposure to light and then fluorescent ternary derivatives can be formed by reaction with aldehydes and primary amines. Over the decades many works and reviews have presented the chemistry developed around ninhydrin [5]. Until now the studies around ninhydrin and its derivatives remained numerous and major, in many areas (e.g. agriculture, biomedical research, applied chemistry) [6,7]. Among all applications using ninhydrin as reagent, quantification of amino acids [8] and fingerprint detection are the most known [9]. Ninhydrin also remains a major reagent for test development [10]. In parallel, ninhydrin is a very important starting material in the design of new polyheterocycles [11]. Moreover, intensive developments in the field of green chemistry (e.g. multicomponent reactions, solvent-free synthesis) use ninhydrin as starting material [12,13]. As shown in Refs. [6c,12], ninhydrin is at the heart of the development of indeno[1,2-*b*]indoles [14]. The use of ninhydrin and substituted ones allowed access to a large library of functionalized indeno[1,2-*b*]indoles with diverse biological activities [15].

In this particular context, some of us has developed numerous ninhydrins to prepare corresponding indeno[1,2-*b*]indoles. To date, ninhydrins have been poorly considered as bioactive molecules as such. Herein, it is for the first time highlighted that such molecules can inhibit hCAs and can be used as lead compounds for the development of inhibitors possessing an innovative mechanism of action. Docking, MM-GBSA and metadynamics calculations [16,17] were used to assess the putative binding mode of this class of underestimated compounds to hCA II and hCA VII, the most physiologically relevant and the most affected CA isoforms, respectively.

2. Results and discussion

2.1. Chemistry

While ninhydrin **2a** was commercially available, all the other tested ninhydrins were synthesised by microwave selenium dioxide oxidation of either the corresponding indan-1-ones **1b-s** [18] for ninhydrins **2b-s** or the tetrabromoindane-1,3-dione **4** for ninhydrin **2t** (Scheme 1). The five new ninhydrins **2d**, **2o**, **2p**, **2s** and **2t**, described herein, were also obtained in good to excellent yields (one at 60% for **2p**, and more than 70% for the other four).

Indan-1-one **1d** [19] was prepared by *O*-alkylation of **1c** [20] by using potassium carbonate (K_2CO_3) and 2-iodopropane in acetone, while indanone **1s** was commercially available. The synthesis of indanones **1o** and **1p** was achieved by electrophilic aromatic substitution in the *para* position of the 4-methoxyindan-1-one **1e** [20]. Introduction of the isopropyl (*i*Pr) group was more difficult to introduce, attempts by using 2-halogenopropane and Lewis acid remaining unsuccessful. Compound **1o** was finally obtained with 41% yield, adding isopropanol (2 eq) to a solution of **1e** (1 eq) in sulfuric acid (2 eq) at 60 °C [21]. For **1p**, the amidomethylation conditions [22] were adapted to both reduce the time reaction and permit its completion. So, a mixture of **1e** (1 eq), 2-chloro-*N*-(hydroxymethyl)acetamide (1.1 eq) in acetic acid/sulfuric acid (ratio 9:1) was microwave irradiated at 70 °C for 10 min to afford **1p** with 84% yield.

Regiochemistry was confirmed by ^{1}H NMR data. Indeed, the presence of the doublet in the aromatic area involved a *ortho* or *para* substitution as expected, due to the orientation effect of the methoxy group. Moreover the chemical shift lower than 7.00 ppm, that is to say at 6.98 ppm for **1o** and 6.95 ppm for **1p**, related to the methoxy effect, was in favour of the *para* substitution. This supposition was confirmed by NOESY and HMBC experiments for **1o** (Fig. 1). In fact, large correlations were observed on the one hand between the methoxy group and H-5 (at 6.98 ppm), and on the other hand between the methyl of the isopropyl group and H-6 (at 7.25 ppm). The same observations were noted in the HMBC spectrum: the carbonyl group only correlated with H-6 ($^4J_{H,C}$) while the methylene group C-2 only correlated with H-5 ($^4J_{H,C}$).

A synthesis path was reported for ninhydrin **2t** [23,24], even if no NMR data was described. In this strategy, ninhydrin **2t** was obtained in two steps from the tetrabromoindane-1,3-dione **3** by using first *p*-toluenesulfonyl azide in the presence of triethylamine and then *tert*-butylhypochlorite in 10% aqueous acetonitrile. So, we decided to adapt our previously reported method [18] to rapidly and easily oxidize indane-1,3-dione **3** into ninhydrin **2t**. Actually, 5 min of microwave irradiation of **3** at 180 °C by using 1.5 eq selenium dioxide afforded ninhydrin **2t** with a good yield of 70% (Scheme 1). Tetrabromoindane-1,3-dione **3** was prepared in two steps from the commercially available tetrabromophtalic anhydride and *tert*-butylacetoacetate [25,26].

2.2. Carbonic anhydrase inhibition

Ninhydrins **2a-t** were investigated as inhibitors of the human CAs I, II, IV, VII and IX by a stopped flow CO_2 hydrase assay. The inhibition data, compared to those of the standard sulfonamide inhibitor acetazolamide (**AAZ**), are reported in Table 1.

The inhibition profiles measured for derivatives **2a-t** indicate that the substitution pattern at the aromatic portion has a great impact on the CA inhibition efficacy of ninhydrins. In fact, compounds **2a-t** resulted to act as low nanomolar to medium micromolar inhibitors depending on the CA isozyme. Interesting structure-activity relationship (SAR) can be worked out. CA II and VII are mostly inhibited in a submicromolar range by ninhydrins **2a-t**. CA II is a cytosolic ubiquitous isoform, whose inhibition is responsible of most side effects of non-selective CAIs. Nonetheless, CA II is abundantly expressed in the brain, as CA VII, and together have been validated as targets for the treatment of CNS-related diseases (e.g. neuropathic pain) [17b]. In detail, inhibition constants (K_Is) against CA VII reach two-digits nanomolar values, making it the most affected CA among those evaluated (K_Is in the range 25–21,300 nM). Notably, only a small pattern of substitutions, that are 5-NO_2 (**2k**), 5-OH (**2m**), 4-OCH_3-7-*i*Pr (**2o**), 5,6-diOCH_3 (**2r**), 4,5,6,7-tetraBr (**2t**), increase two to three-fold the inhibition efficacy of ninhydrin **2a** (K_Is in the range 25–65 nM). Surprisingly, all other substitutions lead to a more or less marked

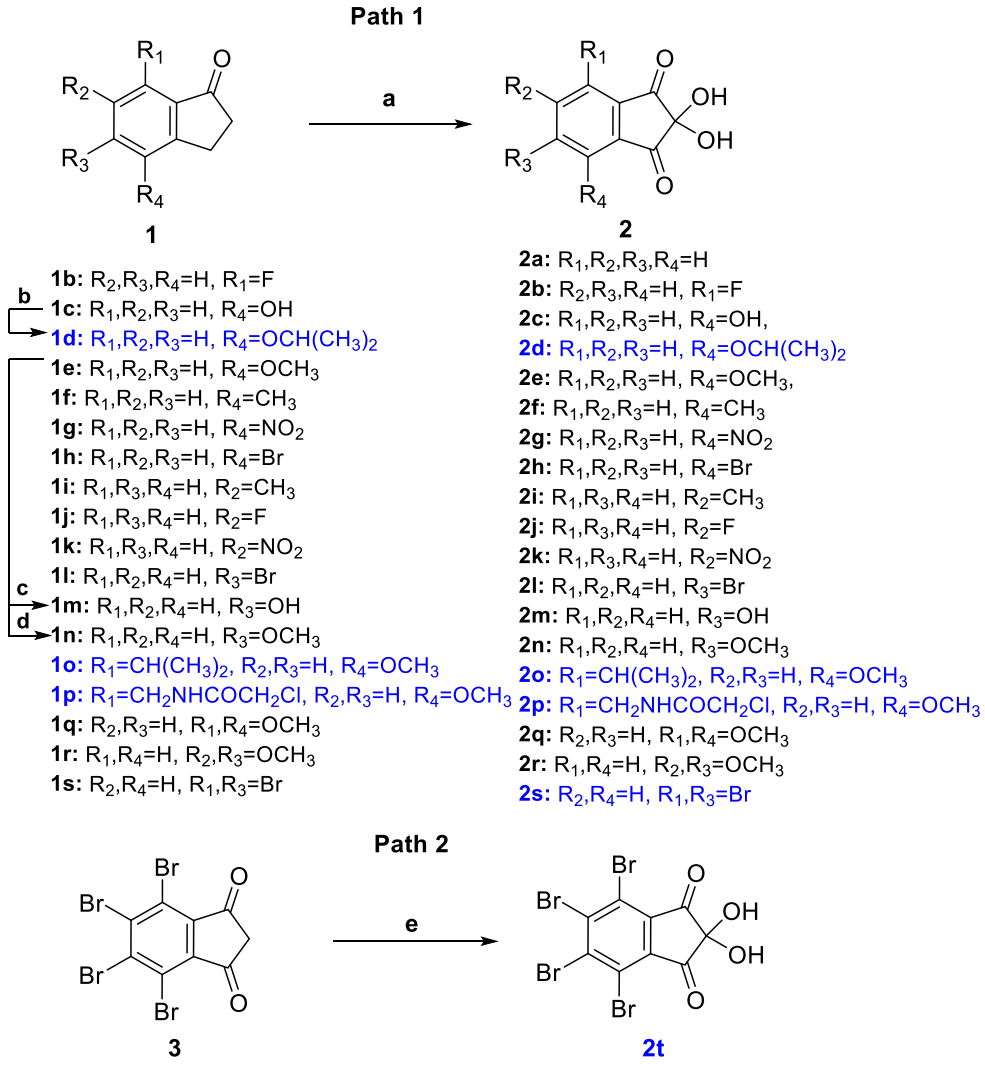

Scheme 1. General ninhydrins **2b-t** syntheses from indan-1-ones **1b-s** or indane-1,3-dione **3**. New compounds described in this article are highlighted blue. **Reagent and conditions: a**). SeO_2, dioxane/water, MW, 5 min, 180 °C, 60–87%; **b**). $(CH_3)_2CHI$, K_2CO_3, acetone, 60 °C, 4 h; 60%; **c**). $(CH_3)_2CHOH$, H_2SO_4, 60 °C, 2 h; 41%; **d**). $ClCH_2NHCOCH_2Cl$, AcOH, H_2SO_4, MW, 70 °C, 10 min, 84%; **e**). SeO_2, dioxane, MW, 5 min, 180 °C, 70%.

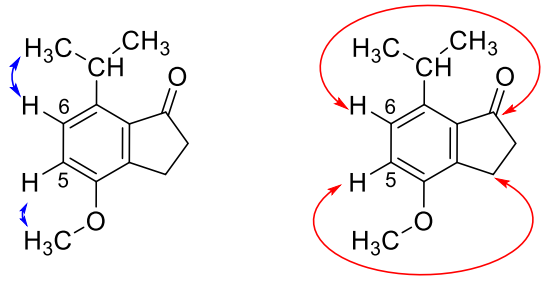

Fig. 1. Significant NOE interactions (in blue) and $^{1}H-^{13}C$ correlations (in red) observed in the NOESY and HMBC spectra of **2o**. (For interpretation of the references to color in this figure legend, the reader is referred to the Web version of this article.)

drop of inhibition efficacy up to more than 2-orders of magnitude (compounds **2d**, **2e**, **2h**, **2i**, **2n**, **2p** are micromolar CA VII inhibitors).

In contrast, ninhydrin **2a** acts as a weak CA II inhibitor (K_Is of 22.7 μM) and only certain investigated substitutions on the aromatic ring increase ninhydrin CA II inhibitory action to a nanomolar range (K_Is in the range 0.20-0.84 μM), that are 4-OH (**2c**), 4-OCH_3 (**2e**), 4-NO_2 (**2g**), 5-F (**2j**), 5-NO_2 (**2k**), 5-OH (**2 m**), 4,7-diOCH_3 (**2q**), 5,6-diOCH_3 (**2r**), 4,5,6,7-tetraBr (**2t**). A few substitutions produced instead a worsening of CA II inhibition, such as in compounds **2i**, **2l**, **2n**, and **2s** (K_Is in the range 26.7-78.2 μM).

CA I and IX are slightly less inhibited by ninhydrins **2a-t** than CA II. In fact, most K_Is against CA I and IX settle in a low micromolar range (1.34–68.2 μM), with the exception of compounds **2e** and **2l** that showed a submicromolar CA I inhibition (K_Is of 0.87 and 0.57 μM). Surprisingly, ninhydrin **2a** resulted the second-best CA IX inhibitor, overcome only by the 4-O*i*Pr derivative **2d** (K_Is 2.37 vs 1.34 μM). Also the bromo-derivatives **2l** and **2t** showed significant single digit micromolar K_Is against CA IX (2.85 and 2.81 μM, respectively).

Interestingly, ninhydrins **2a-t** weakly inhibit (**2i**, **2l**, **2n**, **2t** showed K_Is in the range 39.7–84.6 μM) or did not inhibit CA IV up to a 100 μM concentration.

2.2.1. Molecular modelling

The unsubstituted derivative **2a** was taken as reference compound to investigate the ninhydrin binding mode of the studied derivatives within CAs. Quantum mechanics (QM) derived atom charges were used for docking **2a** within CA II (pdb 5JLT) and CA VII (pdb 3MDZ) active sites. Three top-scored binding poses (bp) for

Table 1
Inhibition data of human CA I, CA II, CA IV, CA VII, CA IX with ninhydrins **2a-t** reported here and the standard sulfonamide inhibitor acetazolamide (**AAZ**) by a stopped flow CO_2 hydrase assay.

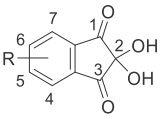

2a-t

Cmpd	R	K_I (μM)[a]				
		CA I	CA II	CA IV	CA VII	CA IX
2a	H	5.38	22.7	>100	0.074	2.37
2b	4-F	8.57	18.4	>100	0.62	44.3
2c	4-OH	16.7	0.73	>100	0.083	17.1
2d	4-O*i*Pr	23.7	6.36	>100	21.3	1.34
2e	4-OCH_3	0.87	0.84	>100	5.36	34.1
2f	4-CH_3	4.86	14.3	>100	1.84	51.4
2g	4-NO_2	26.8	0.41	>100	0.28	31.0
2h	4-Br	6.56	6.39	>100	1.26	61.2
2i	5-CH_3	7.92	49.6	84.6	2.46	16.8
2j	5-F	7.79	0.58	>100	0.27	38.7
2k	5-NO_2	28.4	0.61	>100	0.030	29.6
2l	5-Br	0.57	37.4	71.3	0.39	2.85
2m	5-OH	19.7	0.44	>100	0.065	27.8
2n	5-OCH_3	7.10	78.2	74.3	2.06	13.4
2o	4-OCH_3-7-*i*Pr	36.4	3.12	>100	0.026	54.3
2p	4-OCH_3-7-($CH_2NHCOCH_2Cl$)	8.10	8.90	>100	9.71	8.41
2q	4,7-diOCH_3	8.23	0.35	>100	0.19	68.2
2r	5,6-diOCH_3	41.4	0.20	>100	0.029	30.4
2s	4,6-diBr	36.7	26.7	>100	0.51	2.81
2t	4,5,6,7-tetraBr	4.79	0.26	39.7	0.025	46.7
AAZ	–	0.25	0.012	0.074	0.006	0.025

[a] Mean from 3 different assays, by a stopped flow technique (errors were in the range of ± 5–10% of the reported values).

each CA isoform were computed which exhibit both a tetrahedral zinc-binder character (namely bp1 and bp2 in CA II and bp1 and bp3 in CA VII) and a dual coordination (as trigonal bipyramid) around the metal atom (bp3 in CA II and bp2 in CA VII) (Figs. 2 and 3). Notably, the tetra-coordinated bp establish a series of H-bonds with the residues Thr199 and Thr200 which may involve either the ligand hydroxyl or carbonyl (OH or the CO) groups or both. Additionally, bp1 in CA II features a H-bond between one= CO group of the ligand and H64 side chain. In contrast, a less extended network of H-bonds features the trigonal bipyramid bp where only one (bp3 in CA II, Fig. 2) or two (bp2 in CA VII, Fig. 3) H-bonds are formed with residues Thr199 and Thr200. In all bp, the aromatic portion of ninhydrin **2a** favorably accommodates within the lipophilic binding pocket of CA II and VII, lined by L198, F131, L141, V121, and V143, up to the edge with the hydrophilic active site area represented by Q92.

In order to improve the confidence of the binding mode prediction MM-GBSA score refinement and metadynamics simulations were performed.

First, a MM-GBSA procedure was applied to optimize all six binding modes within the respective CAs active site using the VSGB solvation model and setting the target flexible within 3 Å around the ligand. In CA II, the stability of the binding conformation, measured in term of the computed binding free energy value, reflects the order bp1>bp2>bp3 (Table 2) while bp3 represents the energetically most favored binding orientation in CA VII (−24.53 kcal/mol). The pose stability was assessed with Desmond metadynamics simulations monitoring the fluctuations of the ligand RMSD (Root Mean Square Deviation) over the course of the MD, and the persistence of important contacts, such as hydrogen bonds and π-π interactions, between the ligand and the counterpart including the receptor and any other cofactors or solvent molecules. The RMSD of the simulated ligand with respect to the starting pose, evaluated after the target alignment, was used as the collective variable for the metadynamics simulation. To improve the statistics, 10 simulations have been performed for each bp and the results were averaged over the simulations. Table 2 and Fig. 4 show the outcome of the metadynamics calculations.

The outcomes of the metadynamics (Table 2 and Fig. 4) suggested similar but different **2a** conformations are the most energetically favorable binding poses in CAII (bp1) and CA VII (bp3). This evidence is also confirmed by both the binding persistence (BP) and binding PoseScore (BPS) values, which represent, respectively, the average persistence of contacts and the expectation of the RMSD of the pose over the course of the metadynamics trajectories. The linear combination of these parameters, *i. e* the Binding CompScore (BCS), corroborates the complex stability trend bp1>bp2>bp3 for CA II and bp3>bp1>bp2 for CA VII. These findings lead to the identification of the putative binding conformations of **2a** within the enzyme isoforms (Fig. 5). The narrower active site of CA VII as compared to that one of CA II, well accommodates and stabilizes the **bp3** preferred conformation of compound **2a**, embedding the ligand within its lipophilic cavity better than for **bp2** conformation in CA II.

As shown in Table 1, the incorporation of substituents on the ninhydrin scaffold can thin the inhibition differences existing for **2a** between CA II and VII. Moreover, significant amino acid mutations existing at the edge of CA II and CA VII binding sites (i.e. N67Q, E69D, I91K, L204S) could influence the entrance of the geminal diol derivative having a role in CA VII improved inhibition of **2a** with respect to CA II.

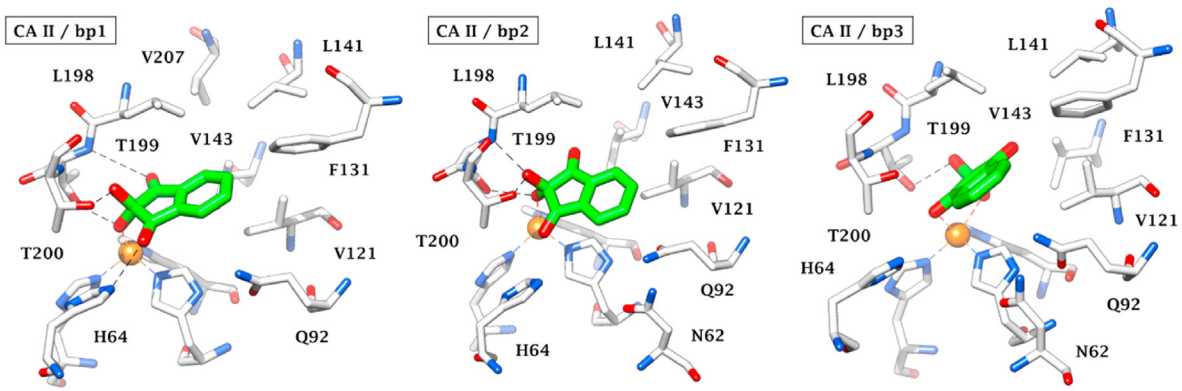

Fig. 2. Top-ranked binding poses for ninhydrin **2a** within CA II active site (pdb 5JLT).

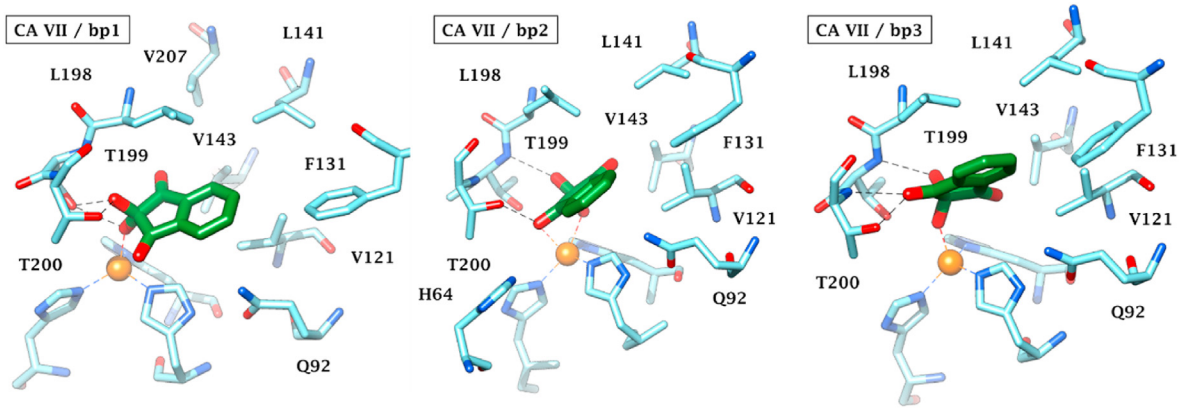

Fig. 3. Top-ranked binding poses for ninhydrin **2a** within CA VII active site (pdb 3MDZ).

Table 2
MM-GBSA derived binding ΔG values and binding pose metadynamics (10 trials average) outcomes with ninhydrin **2a**.

Binding pose (bp)	ΔG binding	BP[a]	BPS[b]	BCS[c]
CA II				
bp1	−28.56	0.377	1.793	−0.094
bp2	−26.14	0.295	2.245	0.768
bp3	−15.58	0.109	2.112	1.566
CA VII				
bp1	−19.26	0.094	2.429	1.959
bp2	−19.84	0.150	3.045	2.295
bp3	−24.53	0.164	1.938	1.120

[a] BP: Binding Persistence, the average persistence of contacts over the course of the metadynamics trajectories. Higher values equate to more stable complexes.
[b] BPS: Binding PoseScore, the expectation of the RMSD of the pose over the course of the metadynamics. Lower values equate to more stable complexes.
[c] BCS: Binding CompScore, the composite score linearly combining the BPS and BP scores. Lower values equate to more stable complexes.

3. Conclusion

Ninhydrin derivatives have an extensive application in organic and applied chemistry and agriculture but have been scarcely investigated in the medicinal chemistry field. Ninhydrin and a series of derivatives substituted on its aromatic ring are here proposed as inhibitors of human carbonic anhydrases (CAs, EC 4.2.1.1), based on earlier evidence that gem diol compounds can coordinate the metal ion from the CA active site. Ninhydrins act as micromolar inhibitors of CA I and IX (K_Is in the range 0.57–68.2 μM) and up to low nanomolar inhibitors against CA II and VII (K_Is in the range 0.025–78.2 μM), recently validated as targets in several CNS-related diseases. CA IV was instead the least affected isoform. A computational protocol composed by docking, MM-GBSA and metadynamics simulations suggested the most putative binding mode of ninhydrin into the active site of CA II and CA VII. The above findings testify that such pharmacologically underestimated ligands may represent interesting lead compounds for the development of CA inhibitors possessing an innovative mechanism of action, which is not very common to other classes of CAIs, i.e., coordination of one or two OH moieties from a diol to the zinc ion from the enzyme active site. In particular, the inhibition profile of ninhydrins, *i.e.* low nanomolar CA VII inhibition *vs* high nanomolar/low micromolar CA II inhibition, make them of relevant interest in the field of CNS-related pathologies that implicate CA (*e.g.* neuropathic pain). In fact, CA II is widespread and ubiquitous in human tissues, whereas CA VII might be considered a CNS-associated enzyme, and its inhibition is expected to induce a minor number of side effects than CA II.

4. Experimental section

4.1. Chemistry

4.1.1. Methods

Chemicals are named according to IUPAC nomenclature. All of the reagents were purchased from Sigma-Aldrich and ThermoFisher Scientific. Microwave reactions were done on a Biotage Initiator Microwave synthesizer 2.0440 W. Melting points were determined on an Electrothermal 9200 capillary apparatus. The IR spectra were recorded on a PerkinElmer Spectrum Two IR spectrometer. The ^{1}H and ^{13}C NMR spectra were recorded at 400 MHz

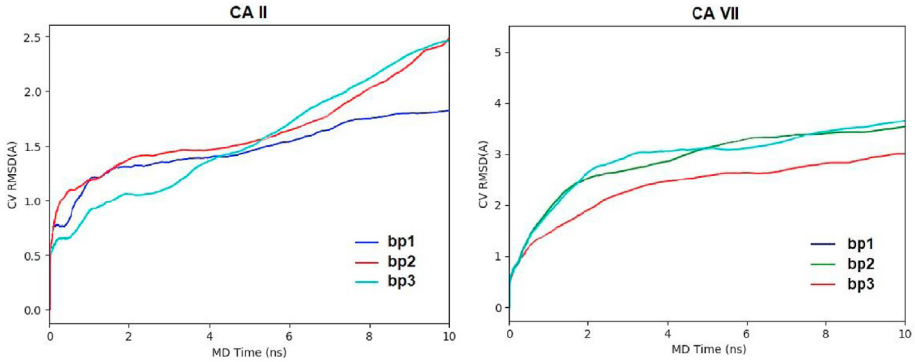

Fig. 4. RMSD average value (10 trials) for **2a** from each of the three initial binding pose per isoform along the simulation course with CA II (left) and CA VII (right).

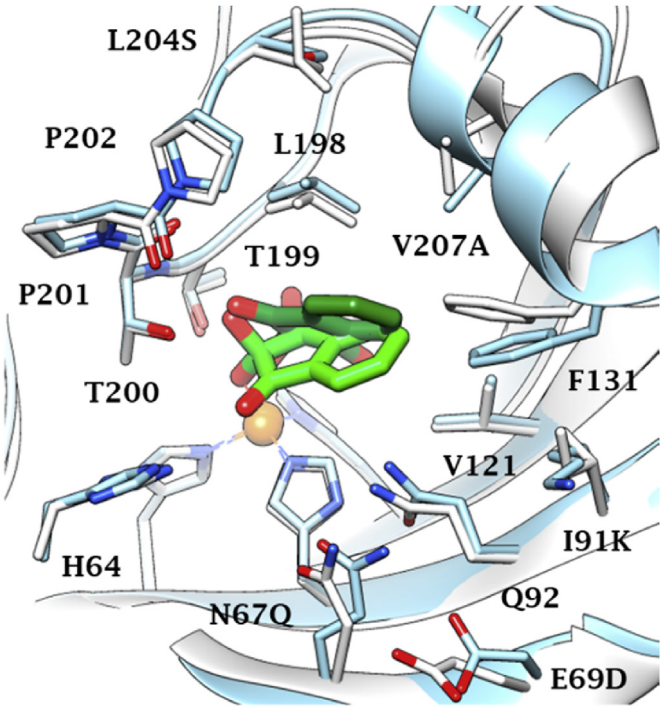

Fig. 5. Superimposition of most stable 2a (light green)/CA II (white) and **2a** (dark green)/CA VII (blue) adducts predicted on the basis of MM-GBSA and metadynamics simulations. L204S, V207A, E69D notations indicate CA II/VII mutated residues. (For interpretation of the references to color in this figure legend, the reader is referred to the Web version of this article.)

on a Bruker DRX 400 spectrometer or at 300 MHz on a Bruker AM 300 spectrometer. Chemical shifts are expressed in ppm (δ) downfield from internal tetramethylsilane and coupling constants J are reported in hertz (Hz). The following abbreviations are used: s, singlet; bs, broad singlet; d, doublet; t, triplet; dd, doubled doublet; q, quartet; qui, quintuplet; sept, septuplet; m, multiplet; Cquat, quaternary carbons. The mass spectra were performed by direct ionization (EI or CI) on a ThermoFinnigan MAT 95 XL apparatus. Chromatographic separations were performed on silica gel columns by column chromatography (Kieselgel 300–400 mesh). All reactions were monitored by TLC on GF254 plates that were visualized under a UV lamp (254 nm). Evaporation of solvent was performed in vacuum with rotating evaporator. The purity of the final compounds (greater than 95%) was determined by uHPLC/MS on an Agilent 1290 system using a Agilent 1290 Infinity ZORBAX Eclipse Plus C18 column (2.1 mm × 50 mm, 1.8 μm particle size) or a Poroshell 120 Agilent infinity lab (2.1 mm × 50 mm, 2.7 μm particle size) with a gradient mobile phase of H_2O/CH_3CN (90:10, v/v) with 0.1% of formic acid to H_2O/CH_3CN (10:90, v/v) with 0.1% of formic acid at a flow rate of 0.5 mL/min, with UV monitoring at the wavelength of 254 nm with a run time of 10 min.

*4.1.2. Synthesis of ninhydrins **2d**, **2o**, **2p** and **2s***

A sealed-pressurised reaction vessel (5 mL) equipped with a magnetic stirrer was charged with indan-1-one (1 eq), selenium dioxide (3.1 eq) and dioxane/water (3 mL/0.3 mL). It was then irradiated with microwave heating to 180 °C with a maximum of 400 W for 5 min. Then, the vessel was rapidly forced-air cooled to room temperature. The mixture was transferred into a round bottom flask, and the vessel washed with acetone. Silica was added to prepare a solid deposit. The volatile solvents were then evaporated *in vacuo* before purification by flash chromatography (ethyl acetate - cyclohexane or dichloromethane - acetone) to afford the corresponding ninhydrin.

*4.1.3. Spectral data of ninhydrins **2d**, **2o**, **2p** and **2s***

*4.1.3.1. 2,2-Dihydroxy-4-isopropoxyindane-1,3-dione (**2d**).* Rf (cyclohexane - ethyl acetate 1:1): 0.28; pink solid; yield: 79%; mp 119–121 °C; **IR** υ (cm^{-1}): 3270 (OH), 1749 (C=O=), 1709 (C=O=); **^{1}H NMR** (400 MHz, DMSO-d_6): δ 7.92 (dd, 1H, J = 8.3 Hz, J = 7.3 Hz, H-6), 7.61 (d, 1H, J = 8.3 Hz, H-7), 7.47 (d, 1H, J = 7.3 Hz, H-5), 7.37 (s, 2H, OH), 4.87 (sept, 1H, J = 6.0 Hz, C<u>H</u>$(CH_3)_2$), 1.35 (d, 6H, J = 6.0 Hz, CH_3); **^{13}C NMR** (100.62 MHz, DMSO-d_6): δ 197.35 (C=O=), 194.27 (C=O=), 156.38 (Cquat), 140.14 (CH), 138.80 (Cquat), 126.15 (Cquat), 121.52 (CH), 114.67 (CH), 87.33 ($C(OH)_2$), 71.29 (OCH), 21.62 ($2CH_3$); **HRMS** calcd for $C_{12}H_{12}NaO_5$ $[M+Na]^+$ 259.0577, found: 259.0571.

*4.1.3.2. 2,2-Dihydroxy-4-isopropyl-7-methoxyindane-1,3-dione (**2o**).* **Rf** (dichloromethane - acetone 9:1): 0.43; yellow solid; yield: 78%; mp 127–129 °C; **IR** υ (cm^{-1}): 3390 (OH), 1740 (C=O=), 1704 (C=O=); **^{1}H NMR** (400 MHz, DMSO-d_6): δ 7.90 (d, 1H, J = 8.8 Hz), 7.55 (d, 1H, J = 8.8 Hz), 7.33 (bs, 2H, OH), 4.03 (m, 1H, C<u>H</u>$(CH_3)_2$), 3.94 (s, 3H, OCH_3), 1.21 (d, 6H, J = 7.1 Hz); **^{13}C NMR** (100.62 MHz, DMSO-d_6): δ 198.41 (C=O=), 194.31 (C=O=), 155.97 (Cquat), 140.66 (Cquat), 136.04 (CH), 134.98 (Cquat), 125.73 (Cquat), 119.91 (CH), 87.01 ($C(OH)_2$), 56.21 (OCH_3), 26.88 (C<u>H</u>$(CH_3)_2$), 22.91 ($2CH_3$); **HRMS** calcd for $C_{13}H_{13}O_4$ $[M\text{-}H_2O + H]^+$ 233.0808, found 233.0812.

*4.1.3.3. 2-Chloro-N-((2,2-dihydroxy-7-methoxy-1,3-dioxoindan-4-yl) methyl)acetamide (**2p**).* Rf (dichloromethane - acetone 7:3): 0.40; beige solid; yield: 60%; mp 118–120 °C; **IR** υ (cm^{-1}): 3359 (OH), 3218 (NH), 1763 (C=O=), 1715 (C=O=), 1669 (C=O=); **^{1}H NMR** (400 MHz, DMSO-d_6): δ 8.75 (t, 1H, J = 5.9 Hz, NH), 7.79 (d, 1H, J = 8.6 Hz, H–Ar), 7.58 (d, 1H, J = 8.7 Hz, H–Ar), 7.41 (bs, 2H, 2OH), 4.70 (d, 2H, J = 5.9 Hz, CH_2NH), 4.17 (s, 2H, CH_2CO), 3.95 (s, 3H, OCH_3); **^{13}C NMR** (100.62 MHz, DMSO-d_6): δ 198.34 (C=O=), 194.31 (C=O=), 166.47 (Cquat), 156.81 (Cquat), 137.44 (CH), 135.59 (Cquat), 130.08 (Cquat), 125.75 (Cquat), 119.69 (CH), 87.11 ($C(OH)_2$), 56.40 (OCH_3), 42.65 (CH_2), 38.55 (CH_2); **HRMS** calcd for $C_{13}H_{11}ClNO_5$ $[M\text{-}H_2O + H^+]^+$ 296.0320, found 296.0329.

*4.1.3.4. 4,6-Dibromo-2,2-dihydroxyindane-1,3-dione (**2s**).* Rf (cyclohexane - ethyl acetate 7:3): 0.57; white solid; yield: 76%; mp 147–149 °C; **IR** υ (cm^{-1}): 3394 (2OH), 1761 (C=O=), 1730 (C=O=), 1182 (C–O); **^{1}H NMR** (400 MHz, DMSO-d_6): δ 8.47 (d, 1H, J = 1.6 Hz, H-5), 8.17 (d, 1H, J = 1.6 Hz, H-7), 7.50 (bs, 2H, OH); **^{13}C NMR** (100.62 MHz, DMSO-d_6): δ 194.11 (C=O=), 193.66 (C=O=), 142.97 (CH), 141.19 (Cquat), 130.83 (Cquat), 129.84 (Cquat), 125.76 (CH), 119.70 (Cquat), 87.13 ($C(OH)_2$); **HRMS** calcd for $C_9H_4Br_2NaO_4$ $[M+Na]^+$ 356.8369, found 356.8371.

*4.1.4. Synthetic procedure of 4,5,6,7-tetrabromo-2,2-dihydroxyindane-1,3-dione (**2t**)*

A sealed-pressurised reaction vessel (20 mL) equipped with a magnetic stirrer and charged with **4** (1.85 g, 4.01 mmol), selenium dioxide (667 mg, 6.01 mmol) and dioxane (15 mL), was irradiated 5 min at 180 °C with a maximum of 400 W. Then, the vessel was rapidly forced-air cooled to room temperature. The mixture was transferred into a round bottom flask, and the vessel washed with acetone. Silica was added to prepare a solid deposit. The volatile solvents were then evaporated *in vacuo* before purification by flash chromatography (ethyl acetate 1/cyclohexane 1) to afford the tetrabromoninhydrin **2t** (1.39 g, 2.81 mmol, 70%).

Rf (cyclohexane - ethyl acetate 2:1): 0.26; red solid; yield: 70%; mp > 160 °C decomposition; **IR** υ (cm^{-1}): 3347 (OH, 1763 (C=O=), 1729 (C=O=), 1163 (C–O); **^{1}H NMR** (300 MHz, DMSO-d_6): δ 7.75 (bs, 2H, OH); **^{13}C NMR** (75 MHz, DMSO-d_6): 192.55 (2=C=O),

139.80 (2Cquat), 137.08 (2Cquat), 121.97 (2Cquat), 86.59 ($C(OH)_2$); **MS-ESI** calcd for $C_9H_2Br_4O_4$ $[M+H]^+$ 490.67, found: 490.70.

4.1.5. Synthetic procedure of 7-isopropyl-4-methoxyindan-1-one (**1o**)

To a stirring solution under argon atmosphere of sulfuric acid (5 mL) at 0 °C, was added portion wise **1e** (500 mg, 3.09 mmol). The mixture was then heated to 60 °C and isopropanol (0.48 mL, 6.18 mmol) rapidly added and left 2 h more stirring. The reaction mixture was then poured into crushed ice and the pH adjusted to approximatively 7 with a 20% aqueous solution of $NaHCO_3$. After extraction of the aqueous layer, with dichloromethane (3 × 30 mL), the combined layers were washed with H_2O, dried over Na_2SO_4, filtered and evaporated under reduced pressure. The obtained residue was purified by flash chromatography (cyclohexane - ethyl acetate 9:1) to afford **1o** (220 mg, 1.08 mmol, 41%).

Rf (cyclohexane - ethyl acetate 9:1): 0.71; yellow solid; yield: 41%; mp 59–61 °C; **IR** υ (cm^{-1}): 1692 (=C=O); **^{1}H NMR** (400 MHz, $CDCl_3$): δ 7.25 (dd, 1H, *J* = 8.3 Hz, *J* = 0.5 Hz, H-6), 6.98 (d, 1H, *J* = 8.3 Hz, H-5), 4.10 (sept, 1H, *J* = 6.9 Hz, C<u>H</u>$(CH_3)_2$), 3.88 (s, 3H, OCH_3), 3.00–2.93 (m, 2H, CH_2CO), 2.69–2.62 (m, 2H, CH_2), 1.23 (d, 6H, *J* = 6.9 Hz, CH(C<u>H</u>$_3)_2$); **^{13}C NMR** (100.62 MHz, $CDCl_3$): δ 207.99 (=C=O), 154.78 (Cquat), 144.80 (Cquat), 141.45 (Cquat), 134.38 (Cquat), 124.89 (CH), 114.73 (CH), 55.48 (OCH_3), 36.94 (CH_2), 26.55 (CH iPr), 23.40 ($2CH_3$), 21.82 (CH_2); **LC-MS** calcd for $C_{13}H_{17}O_2$ $[M+H]^+$ 205.12, found: 205.10.

4.1.6. Synthetic procedure of 2-chloro-N-((7-methoxy-3-oxo-indan-4-yl)methyl)acetamide (**1p**)

A solution of **1e** (2.00 g, 12.3 mmol), acetic acid (9 mL), sulfuric acid (1 mL) and 2-chloro-*N*-(hydroxymethyl)acetamide (1.28 g, 13.5 mmol) was microwave irradiated at 70 °C for 10 min. After cooling, the reaction mixture was transferred in a round bottom flask, the vessel washed with ethyl acetate. Then, silica was added to prepare a solid deposit. The volatile solvents were then evaporated *in vacuo* before purification by flash chromatography (cyclohexane - ethyl acetate 7:3) to afford **1p** (2.76 g, 10.3 mmol, 84%).

Rf (cyclohexane - ethyl acetate 7:3): 0.40; beige solid; yield: 84%; mp 119 °C; **IR** υ (cm^{-1}): 3283 (NH), 1702 (=C=O), 1645 (=C=O); **^{1}H NMR** (400 MHz, $CDCl_3$): δ 7.99 (bs, 1H, NH), 7.32 (d, *J* = 8.1 Hz, 1H, H-6), 6.95 (d, *J* = 8.1 Hz, 1H, H-5), 4.62 (d, *J* = 6.6 Hz, 2H, CH_2NH), 3.97 (s, 2H, CH_2Cl), 3.89 (s, 3H, OCH_3), 3.07–2.99 (m, 2H, CH_2CO), 2.76–2.68 (m, 2H, CH_2); **^{13}C NMR** (100.62 MHz, $CDCl_3$): δ 209.30 (=C=O), 165.98 (N=C=O), 156.98 (Cquat), 146.25 (Cquat), 136.04 (Cquat), 130.31 (CH), 128.31 (Cquat), 114.86 (CH), 55.89 (OCH_3), 43.04 (CH_2), 40.65 (CH_2), 36.86 (CH_2), 22.88 (CH_2); **HRMS** calcd for $C_{13}H_{15}ClNO_3$ $[M+H]^+$ 268.0735, found 268.0733.

4.2. Carbonic anhydrase inhibition

An Applied Photophysics stopped-flow instrument was used for assaying the CA catalyzed CO_2 hydration activity [27]. Phenol red (at a concentration of 0.2 mM) was used as indicator, working at the absorbance maximum of 557 nm, with 10 mM Hepes (pH 7.5) as buffer, 0.1 M Na_2SO_4 (for maintaining constant ionic strength), following the CA-catalyzed CO_2 hydration reaction for a period of 10 s at 25 °C. The CO_2 concentrations ranged from 1.7 to 17 mM for the determination of the kinetic parameters and activation constants. For each inhibitor at least six traces of the initial 5–10% of the reaction have been used for determining the initial velocity. The uncatalyzed rates were determined in the same manner and subtracted from the total observed rates. Stock solutions of activators (10 mM) were prepared in distilled-deionized water and dilutions up to 0.001 μM were done thereafter with distilled-deionized water. The inhibitor and enzyme solutions were preincubated together for 15 min (standard assay at room temperature) prior to assay, to allow for the formation of the E-I complex. The inhibition constant (K_I) was subsequently obtained from the Michaelis-Menten equation, which has been fitted by non-linear least squares using software PRISM 3. Enzyme concentrations in the assay system were in the range of 5–12 nM. The CA isoforms employed were obtained in-house and were recombinant proteins reported earlier by our group [28–30].

4.3. In silico studies

The crystal structure of CA II (pdb 5JLT) [58] and CA VII (pdb 3MDZ) [59] were prepared using the Protein Preparation Wizard tool implemented in Maestro - Schrödinger suite, assigning bond orders, adding hydrogens, deleting water molecules, and optimizing H-bonding networks [46]. Energy minimization protocol with a root mean square deviation (RMSD) value of 0.30 was applied using an Optimized Potentials for Liquid Simulation (OPLS3e) force field. The structure of **2a** was submitted to QM optimization (B3LYP/6-31G*$^+$) and ESP charges calculation with the Jaguar module of Schrödinger [6e]. Grids were centered on the centroids of the co-crystallized ligands and **2a** was docked using QM-computed charges and the standard precision mode (SP). The best poses (bp1-3) within CA II and CA VII, evaluated in terms of score, anchorage, hydrogen bond interactions and hydrophobic contacts, were submitted to optimization and their binding free energies was evaluated by the Prime MM-GBSA protocol [6a], using QM charges and a VSGB solvation model.

Additionally, bp1-3 for both CA II and VII were submitted to metadynamics simulations using Desmond [50] and the OPL3e force field (10 simulations have been performed for each bp). Specifically, the default parameters of the binding pose metadynamics tool implemented in Desmond were used.

Declaration of competing interest

The authors declare that they have no known competing financial interests or personal relationships that could have appeared to influence the work reported in this paper.

Acknowledgements

This work was financially supported in part by the General Directorate for Scientific Research and Technological Development (DG-RSDT), the Algerian Ministry of Scientific Research, the Applied Organic Chemistry Laboratory (FNR 2000) and by the Italian Ministry for University and Research (MIUR), grant PRIN: 2017XYBP2R.

Appendix A. Supplementary data

Supplementary data to this article can be found online at https://doi.org/10.1016/j.ejmech.2020.112875.

References

[1] a) C.T. Supuran, Carbonic anhydrases: novel therapeutic applications for inhibitors and activators, Nat. Rev. Drug Discov. 7 (2008) 168–181;
b) C.T. Supuran, Carbonic anhydrase inhibitors and their potential in a range of therapeutic areas, Expert Opin. Ther. Pat. 28 (2018) 709–712.
[2] (a) C.T. Supuran, Structure and function of carbonic anhydrases, Biochem. J. 473 (2016) 2023–2032;
(b) C.T. Supuran, How many carbonic anhydrase inhibition mechanisms exist? J. Enzym. Inhib. Med. Chem. 31 (2016) 345–360;
(c) A. Nocentini, C.T. Supuran, Advances in the structural annotation of human carbonic anhydrases and impact on future drug discovery, Expet Opin. Drug Discov. 14 (2019) 1175–1197.
[3] (a) V. Alterio, A. Di Fiore, K. D'Ambrosio, C.T. Supuran, G. De Simone, Multiple binding modes of inhibitors to carbonic anhydrases: how to design specific drugs targeting 15 different isoforms? Chem. Rev. 112 (2012) 4421–4468;

(b) N. Pala, R. Dallocchio, A. Dessì, A. Brancale, F. Carta, S. Ihm, A. Maresca, M. Sechi, C.T. Supuran, Virtual screening-driven identification of human carbonic anhydrase inhibitors incorporating an original, new pharmacophore, Bioorg. Med. Chem. Lett 21 (2011) 2515–2520;
(c) G. De Simone, C.T. Supuran, (In)organic anions as carbonic anhydrase inhibitors, J. Inorg. Biochem. 111 (2012) 117–129.

[4] (a) S. Ruhemann, CXXXII.-Cyclic di- and tri-ketones, J. Chem. Soc. 97 (1910) 1438–1449;
(b) S. Ruhemann, CCXII.-Triketohydrindene hydrate, J. Chem. Soc. 97 (1910) 2025–2031.

[5] (a) D.J. McCaldin, The chemistry of ninhydrin, Chem. Rev. 60 (1960) 39–51;
(b) M.M. Joullié, T.R. Thompson, N.H. Nemeroff, Ninhydrin and ninhydrin analogs. Syntheses and applications, Tetrahedron 47 (1991) 8791–8830;
(c) D.B. Hansen, M. Joullié, The development of novel ninhydrin analogues, Chem. Soc. Rev. 34 (2005) 408–417;
(d) G.M. Ziarani, N. Lashgari, F. Azimian, H.G. Kruger, P. Gholamzadeh, Ninhydrin in synthesis of heterocyclic compounds, Arkivoc 2015 (2015) 1–139.

[6] (a) B. Folkertsma, P.F. Fox, Use of the Cd-ninhydrin reagent to assess proteolysis in cheese during ripening, J. Dairy Res. 59 (1992) 217–224;
(b) J.A.W. Jong, M.-E. Moret, M.C. Verhaar, W.E. Hennink, K.G.F. Gerritsen, C.F. van Nostrum, Effect of substituents on the reactivity of ninhydrin with urea, Chemistry 3 (2018) 1224–1229;
(c) S. Sharma, H. Sharma, S. Sharma, S. Paul, V.K. Gupta, N. Boukabcha, A. Chouaih, Triflic acid functionalized carbon@silica composite: synthesis and applications in organic synthesis; DFT studies of indeno[1,2-*b*]indole, Chemistry 5 (2020) 2201–2213.

[7] M. Friedman, Applications of the ninhydrin reaction for analysis of amino acids, peptides, and proteins to agricultural and biomedical sciences, J. Agric. Food Chem. 52 (2004) 385–406.

[8] (a) S. Moore, W.H. Stein, Photometric ninhydrin method for use in the chromatography of amino acids, J. Biol. Chem. 176 (1948) 367–388;
(b) S. Moore, W.H. Stein, A modified ninhydrin reagent for the photometric determination of amino acids and related compounds, J. Biol. Chem. 211 (1954) 907–913;
(c) P.A. Kendall, Use of the ninhydrin reaction for quantitative estimation of amino groups in insoluble specimens, Nature 197 (1963) 1305–1306.

[9] (a) S. Oden, B. Von Hofsten, Detection of fingerprints by the ninhydrin reaction, Nature 173 (1954) 449–450;
(b) C. Champod, C. Lennard, P. Margot, M. Stoilovic, Fingerprints and Other Ridge Skin Impressions, CRC Press, Boca Raton, 2016;
(c) F. Zampa, M. Hilgert, J. Malmborg, M. Svensson, L. Schwarz, A. Mattei, Evaluation of ninhydrin as a fingermark visualisation method - a comparison between different procedures as an outcome of the 2017 collaborative exercise of the ENFSI Fingerprint Working Group, Sci. Justice 60 (2020) 191–200.

[10] (a) M.A. Omar, D.M. Nagy, M.E. Halim, Utility of ninhydrin reagent for spectrofluorimetric determination of heptaminol in human plasma, Luminescence 33 (2018) 1107–1112;
(b) I.M. Mostafa, S.M. Derayea, D.M. Nagy, M.A. Omar, An experimental ninhydrin design approach for the sensitive spectrofluorimetric assay of milnacipran in human urine and plasma, Spectrochim. Acta Mol. Biomol. Spectrosc. 205 (2018) 292–297;
(c) M.R. Lee, C.S. Kim, T. Park, Y.S. Choi, K.H. Lee, Optimization of the ninhydrin reaction and development of a multiwell plate-based high-throughput proline detection assay, Anal. Biochem. 556 (2018) 57–62.

[11] (a) K. Górski, J. Mech-Piskorz, B. Leśniewska, O. Pietraszkiewicz, M. Pietraszkiewicz, Toward soluble 5,10-diheterotruxenes: synthesis and reactivity of 5,10-dioxatruxenes, 5,10-dithiatruxenes, and 5,10-diazatruxenes, J. Org. Chem. 85 (2020) 4672–4681;
(b) A. Upare, N.K. Chouhan, A. Ramaraju, B. Sridhar, S.R. Bathula, Access to pyrrolo[2,1-a]isoindolediones from oxime acetates and ninhydrin via Cu(i)-mediated domino annulations, Org. Biomol. Chem. 18 (2020) 1743–1746;
(c) A.T.A. Boraei, H.A. Ghabbour, A.A.M. Sarhan, A. Barakat, Expeditious green synthesis of novel 4-methyl-1,2,5,6-tetraazafluoranthen-3(2*H*)-one analogue from ninhydrin: N/S-alkylation and aza-Michael addition, ACS Omega 5 (2020) 5436–5442.

[12] (a) B. Jiang, Q.-Y. Li, S.-J. Tu, G. Li, Three-component domino reactions for selective formation of indeno[1,2-*b*]indole derivatives, Org. Lett. 14 (2012) 5210–5213;
(b) X. Chen, Y. Liu, Lactic acid-catalyzed fusion of ninhydrin and enamines for the solvent-free synthesis of hexahydroindeno[1,2-*b*]indole-9,10-diones, Heterocycl. Commun. 22 (2016) 161–163;
(c) M. Kour, M. Bhardwaj, H. Sharma, S. Paul, J.H. Clark, Ionic liquid coated sulfonated carbon@titania composites for the one-pot synthesis of indeno [1,2-*b*]indole-9,10-diones and 1H-pyrazolo[1,2-b]phthalazine-5,10-diones in aqueous media, New J. Chem. 41 (2017) 5521–5532.

[13] H. Karami, Z. Hossaini, M. Sabbaghan, F. Rostami-Charati, One-pot three-component reaction of ninhydrin, 1,3-dicarbonyl compounds, and primary amines to afford indeno[1,2-*b*]pyrrol-4(1*H*)-ones, Chem. Heterocycl. Compd. 54 (2018) 1040–1044.

[14] P. Rongved, G. Kirsch, Z. Bouaziz, J. Jose, M. Le Borgne, Indenoindoles and cyclopentacarbazoles as bioactive compounds: synthesis and biological applications, Eur. J. Med. Chem. 69 (2013) 465–479.

[15] (a) G. Jabor Gozzi, Z. Bouaziz, E. Winter, N. Daflon-Yunes, D. Aichele, A. Nacereddine, C. Marminon, G. Valdameri, W. Zeinyeh, A. Bollacke, J. Guillon, A. Lacoudre, N. Pinaud, S.M. Cadena, J. Jose, M. Le Borgne, A. Di Pietro, Converting potent indeno[1,2-*b*]indole inhibitors of protein kinase CK2 into selective inhibitors of the breast cancer resistance protein ABCG2, J. Med. Chem. 58 (2015) 265–277;
(b) G. Lobo, M. Monasterios, J. Rodrigues, N. Gamboa, M.V. Capparelli, J. Martínez-Cuevas, M. Lein, K. Jung, C. Abramjuk, J. Charris, Synthesis, crystal structure and effect of indeno[1,2-*b*]indole derivatives on prostate cancer in vitro. Potential effect against MMP-9, Eur. J. Med. Chem. 96 (2015) 281–295;
(c) F. Alchab, L. Ettouati, Z. Bouaziz, A. Bollacke, J.-G. Delcros, C.G. Gertzen, H. Gohlke, N. Pinaud, M. Marchivie, J. Guillon, B. Fenet, J. Jose, M. Le Borgne, Synthesis, biological evaluation and molecular modeling of substituted indeno [1,2-*b*]indoles as inhibitors of human protein kinase CK2, Pharmaceuticals 8 (2015) 279–302;
(d) S. Bloch, B. Nejman-Faleńczyk, K. Pierzynowska, E. Piotrowska, A. Węgrzyn, C. Marminon, Z. Bouaziz, P. Nebois, J. Jose, M. Le Borgne, L. Saso, G. Węgrzyn, Inhibition of Shiga toxin-converting bacteriophage development by novel antioxidant compounds, J. Enzym. Inhib. Med. Chem. 33 (2018) 639–650.

[16] V. Limongelli, M. Bonomi, L. Marinelli, F.L. Gervasio, A. Cavalli, E. Novellino, M. Parrinello, Molecular basis of cyclooxygenase enzymes (COXs) selective inhibition, Proc. Natl. Acad. Sci. U.S.A. 107 (2010) 5411–5416.

[17] (a) A. Nocentini, P. Gratteri, C.T. Supuran, Phosphorus versus sulfur: discovery of benzenephosphonamidates as versatile sulfonamide-mimic chemotypes acting as carbonic anhydrase inhibitors, Chem. Eur J. 25 (2019) 1188–1192;
(b) A. Nocentini, V. Alterio, S. Bua, L. Micheli, D. Esposito, M. Buonanno, G. Bartolucci, S.M. Osman, Z.A. ALOthman, R. Cirilli, M. Pierini, S.M. Monti, L. Di Cesare Mannelli, P. Gratteri, C. Ghelardini, G. De Simone, C.T. Supuran, Phenyl(thio)phosphon(amid)ate benzenesulfonamides as potent and selective inhibitors of human carbonic anhydrases II and VII counteract allodynia in a mouse model of oxaliplatin-induced neuropathy, J. Med. Chem. 63 (2020) 5185–5200.

[18] C. Marminon, A. Nacereddine, Z. Bouaziz, P. Nebois, J. Jose, M. Le Borgne, Microwave-assisted oxidation of indan-1-ones into ninhydrines, Tetrahedron Lett. 56 (2015) 1840–1842.

[19] T.M. Kadayat, S. Banskota, G. Bist, P. Gurung, T. Bahadur Thapa Magar, A. Shrestha, J.-A. Kim, E.-S. Lee, Synthesis and biological evaluation of pyridine-linked indanone derivatives: potential agents for inflammatory bowel disease, Bioorg. Med. Chem. Lett 28 (2018) 2436–2441.

[20] W. Liu, M. Buck, N. Chen, M. Shang, N.J. Taylor, J. Asoud, X. Wu, B.B. Hasinoff, G.I. Dmitrienko, Total synthesis of isoprekinamycin: structural evidence for enhanced diazonium ion character and growth inhibitory activity toward cancer cells, Org. Lett. 9 (2007) 2915–2918.

[21] H. Zhang, H. Li, J. Xue, R. Chen, Y. Li, Y. Tang, C. Li, New facile enantio- and diastereo-selective syntheses of (-)-triptonide and (-)-triptolide, Org. Biomol. Chem. 12 (2014) 732–736.

[22] L.M. Oh, H. Wang, S.C. Shilcrat, R.E. Herrmann, D.B. Patience, P. Grant Spoors, J. Sisko, Development of a scalable synthesis of GSK183390A, a PPAR α/γ agonist, Org. Process Res. Dev. 11 (2007) 1032–1042.

[23] C.J. Lennard, P.A. Margot, M. Stoilovic, R.N. Warrener, Synthesis of ninhydrin analogues and their application to fingerprint development: preliminary results, J. Forensic Sci. Soc. 26 (1986) 323–328.

[24] C.J. Lennard, P.A. Margot, M. Stoilovic, R.N. Warrener, Synthesis and evaluation of ninhydrin analogs as reagents for the development of latent fingerprints on paper surfaces, J. Forensic Sci. Soc. 28 (1988) 3–23.

[25] M. Planells, N. Robertson, Naphthyl derivatives functionalised with electron acceptor units - synthesis, electronic characterisation and DFT calculations, Eur. J. Med. Chem. 26 (2012) 4947–4953.

[26] D.R. Buckle, N.J. Morgan, J.W. Ross, H. Smith, B.A. Spicer, Antiallergic activity of 2-nitroindan-1,3-diones, J. Med. Chem. 16 (1973) 1334–1339.

[27] R.G. Khalifah, The carbon dioxide hydration activity of carbonic anhydrase. I. Stop-flow kinetic studies on the native human isoenzymes B and C, J. Biol. Chem. 246 (1971) 2561–2573.

[28] a) A. Innocenti, D. Vullo, A. Scozzafava, C.T. Supuran, Carbonic anhydrase inhibitors. Interactions of phenols with the 12 catalytically active mammalian isoforms (CA I – XIV), Bioorg. Med. Chem. Lett 18 (2008) 1583–1587;
b) L. Menabuoni, A. Scozzafava, F. Mincione, F. Briganti, G. Mincione, C.T. Supuran, Carbonic anhydrase inhibitors. Water-soluble, topically effective intraocular pressure lowering agents derived from isonicotinic acid and aromatic/heterocyclic sulfonamides: is the tail more important than the ring? J. Enzym. Inhib. 14 (1999) 457–474.

[29] A. Nocentini, F. Carta, M. Tanc, et al., Deciphering the mechanism of human carbonic anhydrases inhibition with sulfocoumarins: computational and experimental studies, Chemistry 24 (2018) 7840–7844.

[30] W.M. Eldehna, M.F. Abo-Ashour, A. Nocentini, et al., Enhancement of the tail hydrophobic interactions within the carbonic anhydrase IX active site via structural extension: design and synthesis of novel N-substituted isatins-SLC-0111 hybrids as carbonic anhydrase inhibitors and antitumor agents, Eur. J. Med. Chem. 162 (2019) 147–160.